Supporting Information

Shen et al. 10.1073/pnas.1210417110

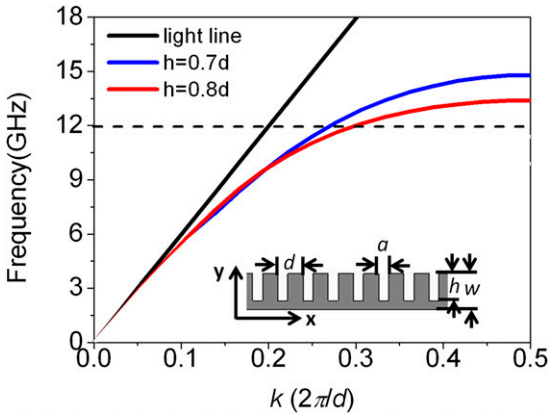

Fig. S1. Dispersion curves for two ultrathin corrugated metal strips ($W = d$, $t = 0.0036d$, $a = 0.4d$, and $d = 5$mm) with different groove depths, $h = 0.7d$ (blue lines) and $h = 0.8d$ (red lines). For the fixed strip width ($W = d$), as the groove depth h increases, the cutoff frequency decreases, and the dispersion curve deviates further from the light line (black line), implying stronger field confinement and enhancement. The horizontal dashed line indicates the frequency of 12 GHz. The wave numbers at this frequency are chosen for the simulations shown in Fig. 2.

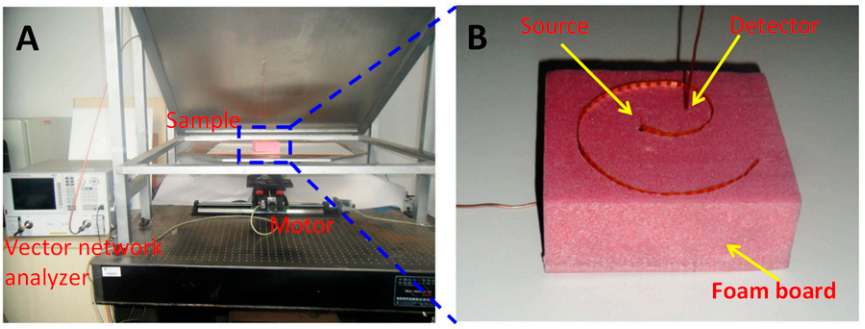

Fig. S2. Photographs of the microwave near-field experiment platform, comprising a planar waveguide (two parallel metal plates), vector network analyzer, source, detector, and motion controller. The CSP structure sample is placed on the movable bottom metal plate, which can move in both the x and y directions, controlled by the motion controller to achieve automated near-electric field scanning with a step resolution of 1 mm. Two electric monopoles with a 0.2-mm-diameter inner conductor and a 1.2-mm-diameter outer conductor were used as the source and detector to excite and probe the electric fields. One port of the vector network analyzer (Agilent N5230C) was connected to the feeding coaxial line to provide the microwave source signal, and the other port was connected to the detecting probe. The detecting probe was fixed onto the upper metal plate to record the E_z components of the E-fields on the observation xy plane, which lies 1.5 mm above the sample. (*A*) Measurement system. (*B*) Measured sample of the spiral CSP structure, showing the source and the detector.

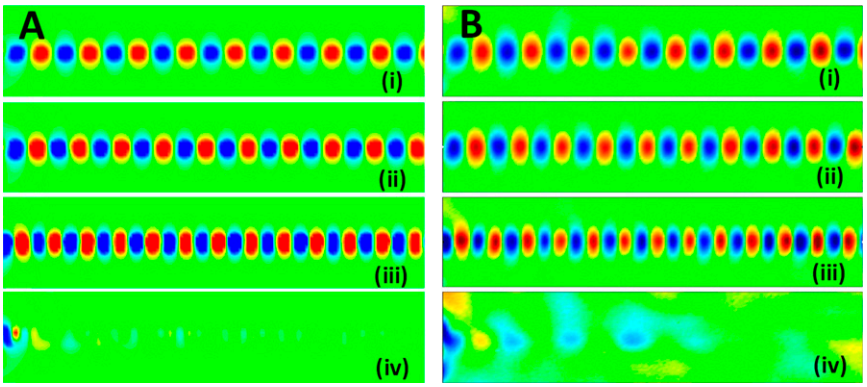

Fig. S3. Simulation (*A*) and measurement (*B*) results of electric field (E_z) distributions at 10 GHz along planar ultrathin corrugated metal films with different groove depths: (i) h = 3 mm; (ii) h = 4 mm; (iii) h = 5 mm; and (iv) h = 6 mm. Here a = 2 mm, d = 5 mm, t = 0.018 mm, and $W = h + 1$ mm. Excellent agreement between the simulation and measurement results is seen. These results demonstrate that the ultrathin corrugated metal strips can confine CSP waves very efficiently in the lateral direction while maintaining the intensities over distances much longer than the wavelength. When the groove depth h increases, the modal wavelength of CSP mode decreases. For the case with h = 6 mm, however, the cutoff frequency is below the operating frequency, and no CSP modes are supported.

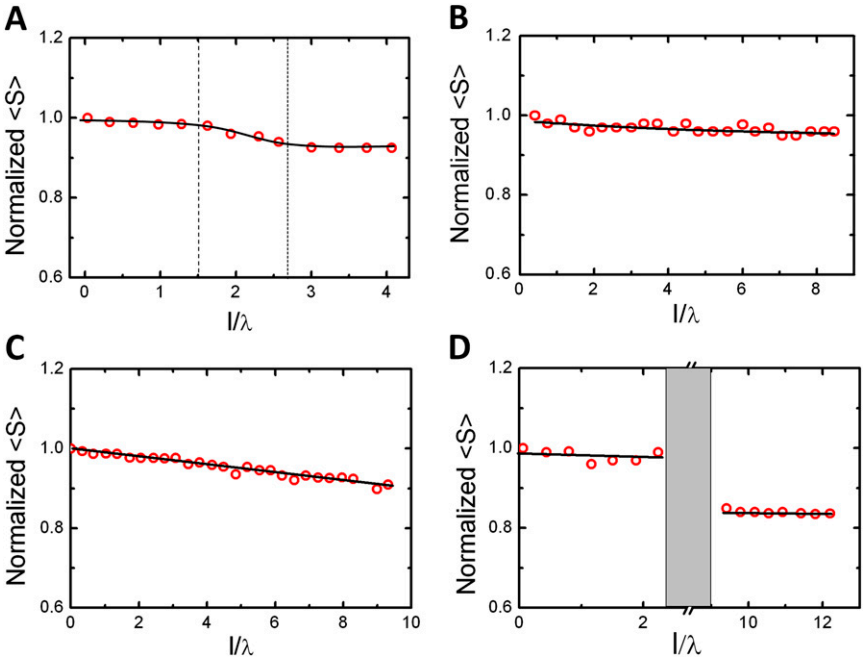

Fig. S4. Normalized time-averaged power density (i.e., the Poynting vector <S≥ 0.5Re[**E**×**H***]) along observation lines (l) that always lies 1.5 mm above the corrugated edges of different CSP structures. (*A*) Planar 60° Y-splitter. Here the observation line is along the main branch and the upper arm, and the first thin dashed line represents the position at which the splitting starts. As shown in Fig. 3 *E* and *F*, the width of CSP mode in each arm is approximately half that of the main branch; thus, the power in each arm is ~42.5% of the total power in the main branch. (*B*) Curved S bending surface. Here the observation is along the curved bending line, and the time-averaged power density at the output side is 95% of that at the input side after passing through nine wavelengths. (*C*) Spiral-shaped CSP surface. Here the observation is along the curved spiral-shaped line, and the time-averaged power density at the output side is 90% of that at the input side after passing through 9.5 wavelengths. (*D*) 3D helix-shaped CSP surface. The shadowed area represents the two-cycle helical route around the dielectric cylinder. The time-averaged power density at the output side is 83% of that at the input side after passing through 12.5 wavelengths.

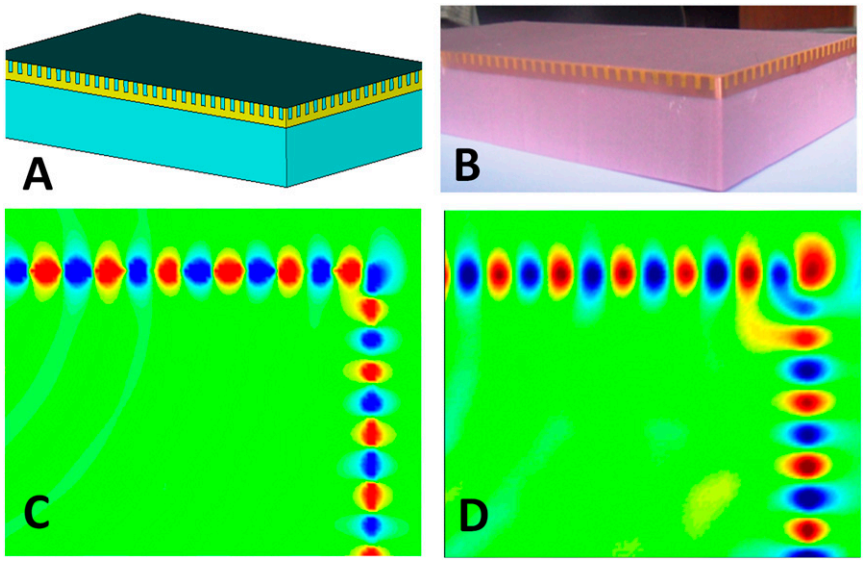

Fig. S5. Propagation of CSP waves on a nonsmooth curved surface (cuboid) at 10 GHz. (*A* and *B*) Designed model and photograph of the fabricated sample, in which a = 2 mm, d = 5 mm, h = 4 mm, W = 5 mm, and t = 0.018 mm. (*C* and *D*) Full-wave simulation (*C*) and experimental (*D*) results of electric field distributions (E_y) on the nonsmooth surface at 10 GHz. The CSP waves can creep through the sharp corner smoothly.

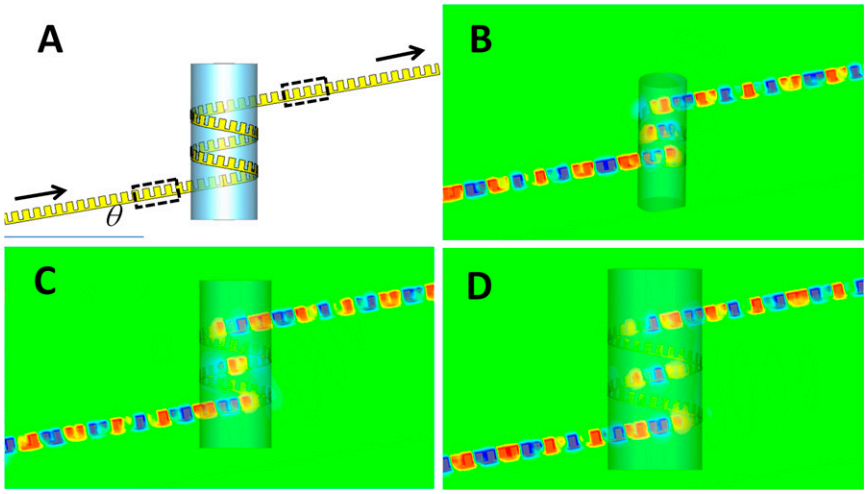

Fig. S6. Full-wave simulation results of near-field distributions (E_z components) at 11 GHz around helix strips of CSP films wrapped on dielectric cylinders of different radii. (*A*) The designed model, in which the comb-shaped ultrathin metal strip is wrapped on the dielectric cylinder forming a helix. The angle between the strip and the horizontal line is 10°, and the arrows indicate the direction of CSP propagation. (*B* and *D*) Full-wave simulation results of electric field distributions (E_z) along the 3D helix paths with different cylinder radii: R_1 = 10 mm (*B*), R_2 = 15 mm (*C*), and R_3 = 20 mm (*D*). The transmission efficiencies are 78% for R_1 = 10 mm, 83% for R_2 = 15 mm, and 81% for R_3 = 20 mm.